




Darcy's law of yield stress fluids on a treelike network

Vincenzo Maria Schimmenti ¹, Federico Lanza ^{1,2}, Alex Hansen ², Silvio Franz,¹ Alberto Rosso,¹ Laurent Talon,³ and Andrea De Luca⁴

¹Université Paris-Saclay, CNRS, LPTMS, 91405 Orsay, France

²PoreLab, Department of Physics, Norwegian University of Science and Technology, N-7491 Trondheim, Norway

³Université Paris-Saclay, CNRS, FAST, 91405 Orsay, France

⁴Laboratoire de Physique Théorique et Modélisation, CY Cergy Paris Université, CNRS, F-95302 Cergy-Pontoise, France



(Received 17 September 2022; accepted 30 June 2023; published 9 August 2023)

Understanding the flow of yield stress fluids in porous media is a major challenge. In particular, experiments and extensive numerical simulations report a nonlinear Darcy law as a function of the pressure gradient. In this letter we consider a treelike porous structure for which the problem of the flow can be resolved exactly due to a mapping with the directed polymer (DP) with disordered bond energies on the Cayley tree. Our results confirm the nonlinear behavior of the flow and expresses its full pressure dependence via the density of low-energy paths of DP restricted to vanishing overlap. These universal predictions are confirmed by extensive numerical simulations.

DOI: [10.1103/PhysRevE.108.L023102](https://doi.org/10.1103/PhysRevE.108.L023102)

In a series of experiments during the nineteenth century, Henry Darcy studied the flow of water in a cylinder filled with sand [1] and established the empirical law for the flow rate Q as a function of the pressure difference P between the two ends of the cylinder

$$Q = \kappa R^2 P / (\eta L), \quad (1)$$

where R and L are, respectively, the radius and the length of the cylinder, and η is the viscosity of the fluid. The permeability, κ , has the dimension of a surface and measures the ability of a given porous medium [2–5] to transmit a fluid. Darcy gave an interpretation of the permeability assuming that, in a medium, the flow is possible only along nonintersecting thin channels, each of radius $R_c \ll R$. The flow along a single channel is given by Poiseuille's law, which holds for empty cylinders and the total flow can be written as $Q = \pi R^2 n^{\text{ch}} \pi R_c^4 P / (8\eta L)$, with n^{ch} the number of channels per unit surface. Hence, the permeability can be identified as $\kappa = \pi n^{\text{ch}} R_c^4 / 8$. The network of the channels of a real porous medium is more complex: channels have heterogeneous shape and can intersect. However, the Darcy law is valid as far as the number of channels remains pressure-independent. This is not the case for yield stress fluids, such as suspensions [6], gels [7], heavy oil [8], slurries, or cement [9] for which a minimum yield stress, σ_y , is needed to flow [10]. Hence, at a low pressure gradient, these yield stress fluids behave like a solid and no flow is measured. However, increasing the pressure gradient, they start flowing along more and more channels. Experiments [11,12] and numerical simulations [13–15] indicated that the Darcy law is modified: below a threshold pressure P_0 no flow occurs, while above it the flow grows nonlinearly with P . Three flowing regimes are observed [16,17]: (1) initially the flow grows linearly in $P - P_0$, but with an effective permeability which is very small; (2) for larger pressure the flow grows nonlinearly as $(P - P_0)^\beta$ (with $\beta \approx 2$) [18,19]; and (3) only above a saturation pressure $P_{\text{sat}} \gg P_0$

does the flow recover the linear growth with the standard permeability κ [20].

Despite these detailed observations, a theoretical explanation for the nonlinearity is still lacking. In this letter we propose an explanation and provide an explicit prediction for the modified Darcy law. We consider a porous structure with the geometry of a binary Cayley tree with t levels (see Fig. 1). This geometry is the simplest with intersecting channels and is realistic for several biological networks (e.g., the alveoli system in the lungs [21] or leaf veins). In this work we establish a precise mapping between the Darcy problem for yield stress fluids and the directed polymer on a Cayley tree, a model displaying one-step replica symmetry breaking (1-RSB) [22,23]. Each individual channel in the porous structure has a pressure threshold which we identify with the energy of the directed polymer represented by that channel. We show that the first channels where flow occurs correspond to those low-energy directed polymers with small overlaps (i.e., they share a short common path). Next we modified the Kolmogorov-Petrovsky-Piskunov (KPP) approach proposed in [24] to determine analytically their number, n^{ch} , as a function of $x = P - P_0$ [see Eq. (13)]. Finally, we determine explicitly the low-pressure behavior, described by Eq. (14), and the linear high-pressure regime of Eq. (15) as well as the saturation pressure P_{sat} [see Eq. (16)]. At this pressure the fluid flows along $\sim t$ channels almost nonoverlapping. By further increasing the pressure, new channels open without significantly changing the permeability of the network. This predictions are confirmed by direct numerical simulations.

Mapping to the directed polymer and large- t limit. Our model is a Cayley tree pore network filled by a Bingham fluid. A pressure P is applied on the root pore and a zero pressure at the leaves. In this model large open pores with a well-defined pressure are connected by tubes of random radius and length. The modified Poiseuille law for a Bingham fluid is an open problem, but in the limit $P \gg \tau$ takes a simple form

$Q_{\text{Pois}}(P) = \frac{\pi R^4}{8\eta L} (P - \tau)_+$ (see [15]). Here we denote $(x)_+ = \max(0, x)$ and $\tau = L\sigma_Y/R$ and consider $P > 0$. We consider the simplified case in which only the thresholds fluctuate and the flow in a tube between the pore i , at the pressure P_i , and the pore j , at pressure $P_j < P_i$, reads

$$Q_{ij} = (P_i - P_j - \tau_{ij})_+. \quad (2)$$

The threshold τ_{ij} is a random variable, drawn from a distribution $p(\tau)$. Hence a tube is open if $P_i - P_j > \tau_{ij}$. A pore has one incoming tube and two outgoing tubes, and inside it Kirchhoff's law holds: the incoming flow must be equal to the sum of the outgoing ones. It follows that, given an open incoming tube, there must be at least one outgoing open tube. Thus along a channel from the root to a leaf flow occurs if all its t tubes are open.

As a consequence, the pressure P_0 at which the first channel opens is given by

$$P_0 = \min_{\alpha} \sum_{(ij) \in \alpha} \tau_{ij}, \quad (3)$$

where α labels the 2^{t-1} directed path connecting the root to a leaf. As observed in [19], the threshold pressure P_0 identifies with the ground-state energy of the associated directed polymer (DP) model. We define ϵ_{α} the energy of a directed path α as the sum of the thresholds along α :

$$\epsilon_{\alpha} = \sum_{(ij) \in \alpha} \tau_{ij}. \quad (4)$$

It follows that $P_0 = \min_{\alpha} \epsilon_{\alpha}$. The key point of this letter is that also the pressures P_1, P_2, \dots at which a new channel opens are related to the low-energy levels of the DP. It is useful to label the directed paths α by ordering the energies as $\epsilon_0 < \epsilon_1 < \epsilon_2 < \dots$.

Using Kirchhoff's law (see Sec. A of [25]) we compute the explicit expression for P_1 :

$$P_1 = \epsilon_0 + \min_{\alpha \neq 0} \frac{\epsilon_{\alpha} - \epsilon_0}{1 - \hat{q}_{0\alpha}/t} = \epsilon_0 + \frac{\epsilon_{\alpha_1} - \epsilon_0}{1 - \hat{q}_{0\alpha_1}/t}, \quad (5)$$

where $\hat{q}_{0\alpha}$ stands for the overlap between the α channel and the ground state, namely, the number of common tubes between the two channels. The path α_1 realizes the minimum, and it is the channel that opens just above P_1 . It is crucial to remark that the minimization involves two terms: the term $\epsilon_{\alpha} - \epsilon_0$ favors low-energy paths, while the term $1/(1 - \hat{q}_{0\alpha}/t)$ selects the ones with a small overlap with the ground state. The directed polymers on a Cayley tree display one-step replica symmetry-breaking 1-RSB. This means that in the limit $t \rightarrow \infty$ the overlap among any two low-energy directed paths is either $O(1)$ or $\sim t$ [22] (finite t corrections are also known [26,27]). Hence, in this large- t limit, the channel α_1 corresponds to a path with low energy and low overlap [$\hat{q}_{0\alpha_1} = O(1)$], so that $\lim_{t \rightarrow \infty} 1/(1 - \hat{q}_{0\alpha_1}/t) = 1$ and $P_1 = \epsilon_{\alpha_1}$. Moreover, the total flow reduces to the sum of the contribution from each channel, namely, $Q_t(P) = (P - P_0)/t + (P - P_1)/t$ for $P \in [P_1, P_2]$ (see Sec. A of [25]).

The same property holds for higher pressures (see Sec. B of [25]): the channels $\alpha_2, \alpha_3, \dots$ correspond to paths with the low energy and low overlap, and P_2, P_3, \dots coincide with the energies $\epsilon_{\alpha_2}, \epsilon_{\alpha_3}, \dots$ (see sorted energies of Fig. 1 bottom).

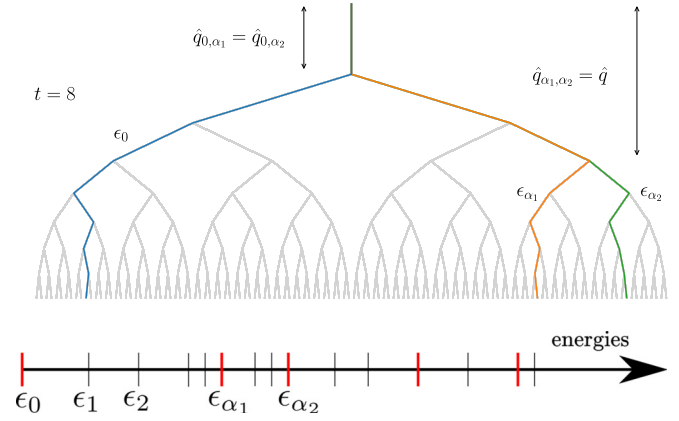


FIG. 1. Top: Binary Cayley tree with $t = 8$ levels. The first channels where flow occur are the leftmost path in blue, at the pressure P_0 , the middle path in orange α_1 , at pressure $P_1 > P_0$, and the rightmost path in green α_2 , at pressure $P_2 > P_1$. We denote with $\hat{q}_{\alpha_1 \alpha_2}$ the overlap between α_1 and α_2 , namely, the length of the common path between them (here $\hat{q}_{\alpha_1 \alpha_2} = 3$). Similarly \hat{q}_{0, α_1} and \hat{q}_{0, α_2} are the overlaps of α_1 and α_2 with the blue path (here $\hat{q}_{0, \alpha_1} = \hat{q}_{0, \alpha_2} = 1$), and \hat{q} is the maximal overlap between all of them (here $\hat{q} = 3$). Bottom: sorted energies of the associated directed polymer $\epsilon_0 < \epsilon_1 < \epsilon_2, \dots$. The energies corresponding to small overlap paths are in red. In the large- t limit we show that $\hat{q} \ll t$ and $P_1 = \epsilon_{\alpha_1}, P_2 = \epsilon_{\alpha_2}, \dots$

Similarly the total flow reduces to the sum of the contribution from each channel.

As a consequence the computation of the flow problem reduces to determine the growth of the number of open channels $n_t^{\text{ch}}(x)$ as a function of $x = P - P_0$. This number identifies with the number of low-energy levels of the directed polymer, provided they have low overlap among them. We compute this number adapting the tools introduced in [24] and based on the mapping to the discrete KPP equation [23,28–32].

KPP approach. To begin, we introduce the number of energy levels with energy smaller than $\epsilon_0 + x$, namely, $m_t^{(\text{full})}(x) = \sum_{\alpha} \vartheta[x - (\epsilon_{\alpha} - \epsilon_0)]$ [$\vartheta(x)$ is the Heaviside theta function]. In [24] (for a self-contained derivation see Sec. B of [25]) $m_t^{(\text{full})}(x)$ (the overbar stands for the average over the random thresholds) is expressed as $m_t^{(\text{full})}(x) = \int dx' r_t(x'; x)$. The function $r_t(x'; x)$ satisfies the following recursive equation:

$$r_{t+1}(x'; x) = 2 \int d\tau p(\tau) \Omega_t(x' - \tau) r_t(x' - \tau; x), \quad (6)$$

$$\Omega_{t+1}(x) = \int d\tau p(\tau) \Omega_t(x - \tau)^2. \quad (7)$$

Here $p(\tau)$ the thresholds distribution and the initial conditions read $r_1(x'; x) = p(x + x')$ and $\Omega_1(x) = \int_x^{\infty} d\tau p(\tau)$. Equation (7) is the discrete KPP equation, and the function $\Omega_t(x)$ is the probability that the ground-state energy of the DP on a Cayley tree of t levels is larger than x . Hence Eq. (7) corresponds to growing a $t + 1$ -level tree starting from two t -level trees [23].

To determine the Darcy flow we are interested in a subset of low-energy paths, namely, the ones that contribute to $n_t^{\text{ch}}(x) = \sum_i \vartheta[x - (P_i - P_0)]$ with $i = 1 \dots 2^{t-1} - 1$. As discussed above, in the limit $t \rightarrow \infty$, the open channels co-

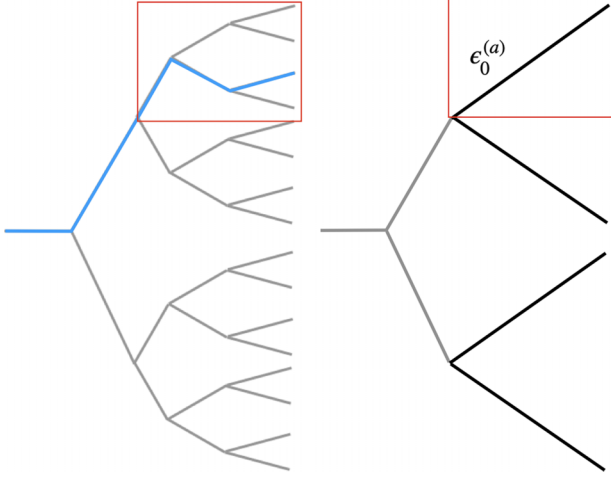


FIG. 2. Left: Example of a Cayley tree. The minimal path of the topmost subbranch after $\hat{q} = 2$ generations is shown highlighted in blue. Right: Pruning of the full Cayley tree, where within each subtree starting from the $\hat{q} = 2$ generation, only the minimal path is retained.

incide with the low-energy paths with vanishing overlap and the pressures P_1, P_2, \dots with the corresponding path energies $\epsilon_{\alpha_1}, \epsilon_{\alpha_2}, \dots$. To make progress we introduce the quantity $m_{\hat{q}}(x)$ which counts, in an infinite tree, the number of paths with energy $\epsilon_{\alpha} \leq P_0 + x$ and the maximum overlap between them \hat{q} . With this prescription, we immediately take limit $t \rightarrow \infty$ and consider only low-energy paths with vanishing overlap, $\hat{q} \ll t$. This remains valid even in the limit $\hat{q} \rightarrow \infty$, so that

$$n_{\infty}^{\text{ch}}(x) = \lim_{\hat{q} \rightarrow \infty} m_{\hat{q}}(x). \quad (8)$$

To compute $\overline{m_{\hat{q}}(x)}$, we modify the KPP approach introduced for $m_t^{(\text{full})}(x)$. For this, we introduce a pruning procedure (see Fig. 2): at the level \hat{q} of the full Cayley tree, there are $2^{\hat{q}}$ subtrees labeled by $a = 1, \dots, 2^{\hat{q}}$. We replace each of these subtrees with a single tube with a minimum energy $\epsilon_0^{(a)}$. In this way we obtain a tree of \hat{q} levels containing the $2^{\hat{q}}$ low-energy paths with maximal overlap \hat{q} . This procedure is equivalent to growing a tree with \hat{q} levels where the leaves thresholds are drawn from the distribution of the minimum of an infinite tree. The probability $w_{\min}(x)$ that the minimal energy of an infinite tree is larger than x is obtained from the fixed-point traveling wave solution of Eq. (7):

$$w_{\min}[x + c(\beta_c)] = \int d\tau p(\tau) w_{\min}^2(x - \tau), \quad (9)$$

where $c(\beta_c)$ is the minimal value for which (9) has a solution and its value can be obtained as

$$\beta_c = \arg \min_{\beta} c(\beta), \quad (10a)$$

$$c(\beta) = \frac{1}{\beta} \log \left(2 \int d\tau p(\tau) e^{-\beta\tau} \right). \quad (10b)$$

The function $w_{\min}(x)$ is a sigmoid with $w_{\min}(x) \simeq 1 - x \exp(\beta_c x)$ for $x \rightarrow -\infty$ and $w_{\min}(x) \simeq 0$ for $x \rightarrow \infty$. The

solution of Eq. (9) is defined up to an arbitrary shift that we set to zero for simplicity. For large but finite t , it has been proven [33] that

$$P_0 = \epsilon_0 = -c(\beta_c)t + \frac{3}{2\beta_c} \log t + \chi_0, \quad (11)$$

where the first two terms are deterministic while χ_0 is a random variable of order 1 distributed according to $-w'_{\min}(\chi_0)$. In our problem, the limit $t \rightarrow \infty$ can be safely taken as the divergent deterministic part being unimportant, being the same for all leaves.

Thus, to compute $\overline{m_{\hat{q}}(x)}$, one has to implement the recurrence in \hat{q} instead of t , replacing $r_t(x'; x)$ with $r_{\hat{q}}(x'; x)$. Moreover, in Eq. (6), $\Omega_t(x)$ is replaced with $w_{\min}[x + c(\beta_c)\hat{q}]$ and the initial condition is $r_{\hat{q}=1}(x'; x) = -w'_{\min}(x + x')$. Finally, as before, $\overline{m_{\hat{q}}(x)} = \int dx' r_{\hat{q}}(x'; x)$.

In the limit $t \rightarrow \infty$ a closed-form expression for $m_{\infty}^{(\text{full})}(x)$ is not known [34]; however, in [24] it was shown numerically that the following asymptotic holds:

$$\overline{m_{\infty}^{(\text{full})}(x)} \stackrel{x \gg 1}{\simeq} A x e^{\beta_c x} \quad (12)$$

with A a nonuniversal $O(1)$ constant. On the contrary, direct numerical integration of $r_{\hat{q}}(x'; x)$ [Fig. 3 (right)] show that, when $\hat{q} \rightarrow \infty$, the expression of $n_{\infty}^{\text{ch}}(x)$ is

$$n_{\infty}^{\text{ch}}(x) = \lim_{\hat{q} \rightarrow \infty} \overline{m_{\hat{q}}(x)} = e^{\beta_c x}. \quad (13)$$

In [25], we also provide an analytical argument to support this result.

Determination of the flow. At low pressure, for a fixed $x = P - P_0$, there is a finite number of channels, sharing low overlap and each supporting a flow $(x - x')/t$, $P_0 + x'$ being its opening pressure. In this regime the total flow reduces the sum of independent contributions $Q_t(P_0 + x) = \int_0^x dx' n_t^{\text{ch}}(x - x')/t$. For large t this leads to

$$\overline{Q_t(P_0 + x)} = \frac{e^{\beta_c x} - 1}{\beta_c t} \quad \text{with } P \gtrsim P_0. \quad (14)$$

This expression captures the first two regimes of the flow: when $P \rightarrow P_0$ the flow is linear $Q(P) = (P - P_0)/t$, for larger pressure a nonlinear regime takes over. At very high pressure instead all channels are open, and we recover the second linear behavior with

$$Q_t(P) = \kappa(P - P^*) \quad \text{with } P \rightarrow \infty. \quad (15)$$

For large t , $\kappa = 1/2$ and $P^* = \bar{\tau}t$ [with $\bar{\tau} = \int \tau p(\tau) d\tau$; see Sec. C of [25]].

The crossover between the nonlinear regime of Eq. (14) and the linear regime of equation (15) occurs at the pressure P_{sat} . An estimation of P_{sat} is obtained by matching the effective permeability at low pressure, $\overline{\kappa_{\text{eff}}} = d\overline{Q_t}/dP \sim e^{\beta_c(P - P_0)}/t$, with the value $\kappa = 1/2$ at high pressure:

$$P_{\text{sat}} = P_0 + (1/\beta_c) \ln t. \quad (16)$$

As a consequence, at the saturation pressure, the number of channels obtained by Eq. (13) is $\sim t$. Let us comment on this result. When the pressure is slightly above the minimal value P_0 , only a single channel is open and κ_{eff} is $\sim 1/t$. Increasing

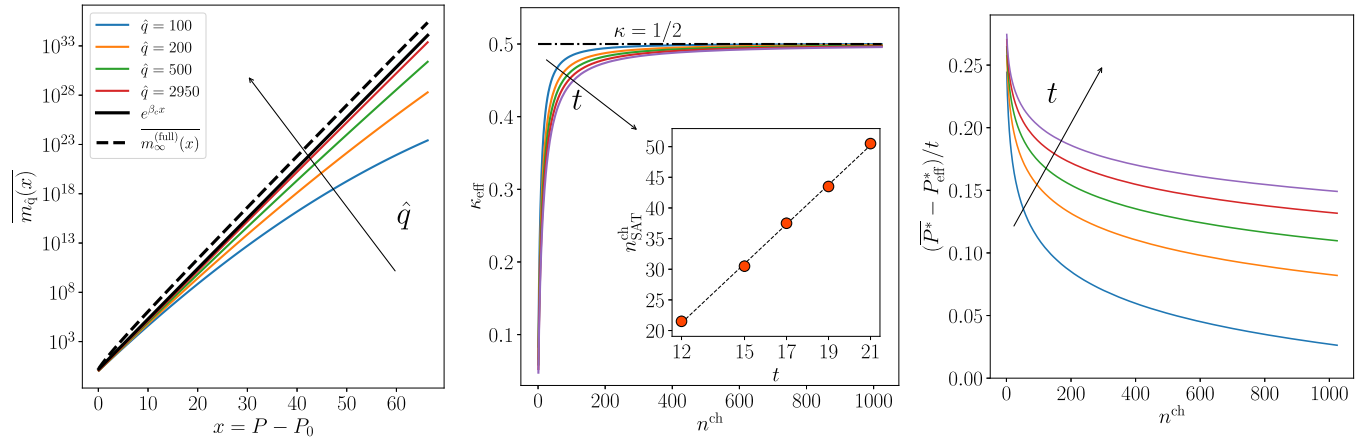


FIG. 3. Left: $\overline{m_{\hat{q}}(x)}$ and $\overline{m_{\infty}^{(full)}}(x)$ (dashed black line) obtained by numerical integration of Eq. (6) and Eq. (7) with different initial conditions. Middle and right: exact numerical simulations on a finite Cayley tree of moderate moderate sizes $t = 12, 15, 17, 19, 21$. The opening of the first $\sim t$ channels is sufficient to saturate the effective permeability, $\kappa_{\text{eff}}(n_{\text{SAT}}^{\text{ch}}) = 0.4 = 0.8\kappa$ (inset). However, P_{eff}^* displays a much slower evolution, and it is still far from saturation when $n^{\text{ch}} \sim 1000 \gg t$. The simulations were carried out using a Gaussian distribution $p(\tau)$ with zero mean and variance $\sigma^2 = 1/12$. The corresponding value for β_c from (10) is $\beta_c = \sqrt{2 \ln 2}/\sigma$.

the pressure slightly more ($\sim \ln t$), it is enough to have $\sim t$ channels with very small overlap between them and to reach the total permeability κ . Note that this number is very small compared to 2^{t-1} , the total number of directed paths. At even larger pressure, the fluid flows in more and more channels, but this does not affect much the permeability of the network. To check these results we carried out exact numerical simulations on the Cayley tree with moderate t . For a given finite tree the flow curve as function of the pressure is a piecewise linear function, with breakpoints at $P_0, P_1, \dots, P_{n^{\text{ch}}}$, the pressures at which a new channel opens. For each segment the flow reads $Q(P) = \kappa_{\text{eff}}(P - P_{\text{eff}}^*)$. The first parameter, κ_{eff} , is the permeability of the set of open channels, while P_{eff}^* depends on the threshold along them. In Fig. 3 we study their behavior as a function of n^{ch} . In Fig. 3 (middle), we observe that the permeability grows quickly with n^{ch} and after $n_{\text{SAT}}^{\text{ch}} \sim t$ reaches the value $\kappa = 1/2$ [see the inset of Fig. 3 (middle)]. The converse is not true for P_{eff}^* , which grows slowly as shown in Fig. 3 (right).

Conclusions. In this work we show that the Darcy problem with a yield stress fluid is closely related to the associated directed polymer. In particular, in the limit of large trees, a direct mapping emerges between n^{ch} and low-energy directed paths with zero overlap. Due to this identification, we derive a simple universal expression for the flow as a function of the applied pressure. Equation (14) is independent of most microscopic details. However, the threshold distribution and the tree branching ratio set the parameter β_c .

The next big challenge would be to solve the problem of the flow in a finite dimension. In particular, it would be interesting to understand the role of the low-energy and

low-overlap energy levels. Those low-overlap excitations are abundant in mean-field glassy disordered systems, but their number is suppressed in a finite dimension. For this reason, their role in realistic setups has always been controversial. However, in the Darcy problem, excitations with high overlap are strongly penalized, and they are inessential in increasing the flow, independently of the spatial dimension. For this reason, the Cayley tree solution of the flow can give important insights on finite dimensional porous media. In particular the high-pressure behavior of Eq. (15) holds in all dimensions, and we expect that the scenario depicted in Fig. 3 (middle and right) holds as well. In a real porous medium, we predict that the effective permeability grows initially fast and saturates to κ , while P_{eff}^* evolves slowly to $P^* = t\bar{\tau}$. Moreover, from the Cayley tree solution, we know that the permeability of the network of flowing channels is governed by a small number of independent channels. It would be interesting to understand if this remains true in finite dimensions.

Acknowledgments. We thank X. Cao and V. Ros for discussions and suggestions. A.D.L. acknowledges support by the ANR JCJC grant ANR-21-CE47-0003 (TamEnt). We acknowledge the support of the Simons Foundation (Grant No. 454941, S.F.). This work was partly supported by the Research Council of Norway through its Center of Excellence funding scheme, Project No. 262644. Further support, also from the Research Council of Norway, was provided through its INTPART program, Project No. 309139. This work was also supported by Investissements d’Avenir du LabEx PALM (ANR-10-LABX-0039-PALM), V.S. acknowledges 80Prime CNRS support for the project CorrQuake.

[1] H. Darcy, *Les Fontaines Publiques De La Ville De Dijon* (Victor Dalmont, Paris, 1856).

[2] J. Bear, *Dynamics of Fluids in Porous Media* (Dover, Paris, 1988).

- [3] M. Sahimi, *Flow and Transport in Porous Media and Fractured Rock: From Classical Methods to Modern Approaches* (Wiley, Paris, 2011).
- [4] M. J. Blunt, *Multiphase Flow in Permeable Media* (Cambridge University Press, 2017).
- [5] J. Feder, E. G. Flekkøy, and A. Hansen, *Physics of Flow in Porous Media* (Cambridge University Press, Paris, 2022).
- [6] A. Fall, F. Bertrand, G. Ovarlez, and D. Bonn, *Phys. Rev. Lett.* **103**, 178301 (2009).
- [7] J. Piau, *J. Non-Newtonian Fluid Mech.* **144**, 1 (2007).
- [8] H. Pascal, *Acta Mech.* **39**, 207 (1981).
- [9] P. Coussot, *Rheometry of Pastes, Suspensions, and Granular Materials: Applications in Industry and Environment* (John Wiley and Sons, Paris, 2005).
- [10] E. Bingham, *Fluidity and Plasticity* (McGraw-Hill, New York, 1922).
- [11] T. Al-Fariss and K. L. Pinder, *Can. J. Chem. Eng.* **65**, 391 (1987).
- [12] G. Chase and P. Dachavijit, *Rheol. Acta* **44**, 495 (2005).
- [13] X. Lopez, P. H. Valvatne, and M. J. Blunt, *J. Colloid Interface Sci.* **264**, 256 (2003).
- [14] M. T. Balhoff and K. E. Thompson, *AIChE J.* **50**, 3034 (2004).
- [15] M. Chen, W. Rossen, and Y. C. Yortsos, *Chem. Eng. Sci.* **60**, 4183 (2005).
- [16] L. Talon and D. Bauer, *Eur. Phys. J. E* **36**, 139 (2013).
- [17] T. Chevalier and L. Talon, *Phys. Rev. E* **91**, 023011 (2015).
- [18] S. Roux and H. J. Herrmann, *Europhys. Lett.* **4**, 1227 (1987).
- [19] C. Liu, A. De Luca, A. Rosso, and L. Talon, *Phys. Rev. Lett.* **122**, 245502 (2019).
- [20] H. Barnes, *A Handbook of Elementary Rheology* (University of Wales, Institute of Non-Newtonian Fluid Mechanics, Aberystwyth, Wales, 2000).
- [21] B. Mauroy, M. Filoche, E. R. Weibel, and B. Sapoval, *Nature (London)* **427**, 633 (2004).
- [22] M. Mézard, G. Parisi, and M. A. Virasoro, *Spin Glass Theory and Beyond: An Introduction to the Replica Method and Its Applications* (World Scientific Publishing Company, Paris, 1987).
- [23] B. Derrida and H. Spohn, *J. Stat. Phys.* **51**, 817 (1988).
- [24] É. Brunet and B. Derrida, *J. Stat. Phys.* **143**, 420 (2011).
- [25] See Supplemental Material <http://link.aps.org/supplemental/10.1103/PhysRevE.108.L023102> for additional information about each of the three sections of the main paper: mapping to the directed polymer and large- t limit (Sec. A), the KPP approach (Sec. B), and determination of the flow (Sec. C).
- [26] B. Derrida and P. Mottishaw, *Europhys. Lett.* **115**, 40005 (2016).
- [27] X. Cao, A. Rosso, R. Santachiara, and P. Le Doussal, *Phys. Rev. Lett.* **118**, 090601 (2017).
- [28] S. N. Majumdar and P. Krapivsky, *Physica A* **318**, 161 (2003).
- [29] S. N. Majumdar and P. L. Krapivsky, *Phys. Rev. E* **62**, 7735 (2000).
- [30] S. N. Majumdar and P. L. Krapivsky, *Phys. Rev. E* **65**, 036127 (2002).
- [31] L.-P. Arguin, A. Bovier, and N. Kistler, *Commun. Pure Appl. Math.* **64**, 1647 (2011).
- [32] K. Ramola, S. N. Majumdar, and G. Schehr, *Chaos, Solitons, Fractals* **74**, 79 (2015).
- [33] M. Bramson, *Convergence of Solutions of the Kolmogorov Equation to Traveling Waves* (American Mathematical Soc., 1983), Vol. 285.
- [34] X. Cao, Y. V. Fyodorov, and P. L. Doussal, *SciPost Phys.* **1**, 011 (2016).